Synthesis of Carbon Nanotubes on Cerium-Substituted Barium Ferrite Substrate by Chemical Vapor Deposition for Preparation of a Microwave Absorbing Nanocomposite

Pourabdollahi, Hakimeh; Zarei, Ali Reza*[+]

Faculty of Chemistry and Chemical Engineering, Malek Ashtar University of Technology, P.O. Box 15875-1774 Tehran, I.R. IRAN

ABSTRACT: *In this research, at first, Ce-substituted barium ferrite, $BaCe_{0.2}Fe_{11.8}O_{19}$ was prepared via the sol-gel method as a substrate and then Carbon NanoTubes (CNTs) was synthesized on the surface of the substrate by Chemical Vapor Deposition (CVD) technique. The structure, morphology, and electromagnetic performance of the synthesized nanocomposites were characterized by XRD, FE-SEM, and Vibrating Sample Magnetometer (VSM), respectively. The results indicated that the $BaCe_{0.2}Fe_{11.8}O_{19}$ particles were coated by CNTs, and the nanocomposite has magnetic properties. Therefore, the electromagnetic properties including complex permittivity (ε_r), the permeability (μ_r), and microwave absorption properties were investigated using a vector network analyzer. It was found that in the nanocomposite, because of the presence of CNTs, the Reflection Loss (RL) widely increased. The maximum reflection loss in the frequency range of 8-12 GHz for 2.5 mm thickness was -49.61 dB at 9.0 GHz. The results suggest that prepared nanocomposite can be suitable in the microwave absorbing coatings.*

KEYWORDS: *Chemical vapor deposition; Carbon nanotubes; Barium ferrite; Microwave absorbing material; Reflection loss.*

INTRODUCTION

Increasing scientific interest and advancement of ElectroMagnetic (EM) wave absorbing materials have been extended because of EM interference problems. Radar Absorbing Materials (RAMs) in the microwave frequency range are interested because of their applications in the aircraft stealth, anti-electromagnetic interference coating, microwave thermal seed materials, and military protecting [1-4]. They can absorb EM waves via three absorbing mechanisms including the dielectric loss, the magnetic loss and the conductive loss and then convert EM energy into thermal energy or dissipate microwaves by interference [5, 6]. The conjugation of dielectric materials and magnetic materials could be an effective way to obtain excellent impedance matching, which is expected to achieve excellent microwave absorption [7-9]. Based on the magnetic or dielectric loss, a variety of EM wave absorbing materials have been designed and developed such as magnetic metal powders, ferrite, ceramics, conducting polymers, carbon-based materials, etc. [10-16].

***** *To whom correspondence should be addressed.*
+ E-mail: zarei1349@gmail.com
1021-9986/2020/1/1-10 10/$/6.00

Among the different materials, hexagonal ferrites with super chemical stability, high anisotropic field, high saturation magnetization, the critical value of permeability, and planar anisotropic behavior in microwave frequencies are appropriate as RAM. The hexagonal-type ferrite absorbs microwave energy by losing interaction of the magnetic field of the wave with their individual magnetization [17, 18]. Barium ferrites, which possess large saturation magnetization and high natural resonance frequency have been notable as uncommon sorts of absorbing materials [19, 20].

It is well known that the dielectric and magnetic properties can be modulated by substitution of Fe^{+3} and Ba^{+2} ions with other ions [21, 22]. Due to typical relaxation characterization, Rare Earth Elements (REs) may affect the electromagnetic properties of ferrites [23]. Recent investigations have shown that saturation magnetization, coercivity and anisotropy are improved after Ba^{+2} or Fe^{+3} ion is substituted by REs, which results in the change of the magnetic interactions [24]. Furthermore, in addition to lower complex permittivity, RE-substituted ferrites, present lesser matching thickness, larger bandwidth and obvious relaxation that contributes to improving impedance matching, compared to those without substitution [25]. The cerium element (Ce) is known as a dopant applied in the field of microwave absorbers [26].

Carbon Nanotubes (CNTs) as conductive filler have been investigated in RAMs, due to their physical and chemical properties such as light weight and strong microwave absorption properties in the GHz frequency range [27, 28]. Although CNTs do not indicate magnetic loss during microwave absorption, their absorption characteristics are limited, but could be improved by using low decorating ratios of magnetic materials. CNTs are regularly designed with magnetic materials to modify their magnetization, such as coating or filling with ferromagnetic and super para magnetic materials [29]. Nanocomposite of CNTs and inorganic microwave absorbing materials combines better-matched impedance characteristics and improved reflection loss of both materials. It has been reported that combination of CNTs with hexaferrites enhanced the magnetic properties of the carbon nanotubes [30-34].

There are several methods for the production of carbon nanotubes with metallic or semi-conducting properties. The most well-known utilized strategies for the creation of nanotubes are arc discharge, laser vaporization, and Chemical Vapor Deposition (CVD). The CVD technique is appropriate for CNTs growth at large scale and high purity with low costs for applied application [35,36]. There are many hydrocarbons such as methane, natural gas, acetylene, and benzene are carbon sources which are widely used for synthesis of CNTs [37]. CVD synthesis of CNTs requires the metal as catalysts. Catalysts play a very important function and the quality of CNTs can be modified by improving the desired characteristics. Catalyst particles act as nucleation sites for CNT growth. The role of the catalyst is to decompose hydrocarbons at lower temperature than the spontaneous decomposition temperature of hydrocarbon via heat and its new nucleation to form CNTs. The pure CNTs can be prepared by hydrocarbon decomposition on the catalysts surface, such as noble metals, ceramic nanoparticle catalysts and semiconducting nanoparticles [38-43].

In this work, we have developed a method for preparation of a magnetic ferrite-CNTs nanocomposite. At first, Ce-substituted barium ferrite substrate, $BaCe_{0.2}Fe_{11.8}O_{19}$, was synthesized via sol-gel method, followed by coated with carbon nanotube produced *via* CVD by using methane gas as carbon source. Thus, the structural and magnetic characteristics of the prepared nanocomposite were evaluated.

EXPERIMENTAL SECTION

Reagents

All the reagents for the synthesis of Ce-substituted barium ferrite including barium nitrate $Ba(NO_3)_2.6H_2O$, iron(III) nitrate ($Fe(NO_3)_3.9H_2O$), and cerium nitrate ($Ce(NO_3)_3.6H_2O$) with analytical grade were purchased from Merck (Darmstadt, Germany) and deionized water (DI) was used throughout the study.

Instruments

The phase of powders was estimated by X-ray diffraction (XRD) patterns were recorded by a Philips-X'pertpro X-ray diffractometer using Cu Ka radiation (λ= 1.54 Å). FE-SEM images were acquired using an electron microscopy Sigma model (Zeiss Ltd. Co., Germany). The magnetic properties were measured by using a vibrating sample magnetometer (VSM, TM-XYZTB-SIH). The electromagnetic parameters

were measured by an Agilent 8510C network analyzer in the range of 8–12 GHz.

Preparation of substrate

Ce-substituted barium ferrite was prepared by the sol–gel method. A stoichiometric amount of $Ba(NO_3)_2.6H_2O$, $Fe(NO_3)_3.9H_2O$ and $Ce(NO_3)_3.6H_2O$ was dissolved in a citric acid aqueous solution under stirring. The molar ratio of nitrates to citric acid was 1:1. Then, an appropriate amount of ammonia hydroxide solution was dropped into the solution under continuous stirring to adjust the pH value to about 7. The precursor mixture was heated by a water bath at 80 ºC under stirring for 3 h. Then, it was dried in a drying box at 120 ºC until the gel formed. The dried gel was calcined at 210 ºC in a silicon carbide furnace in air so as to remove the organic substance. Finally, the $BaCe_{0.2}Fe_{11.8}O_{19}$ powder was obtained after the sample was treated at 900 ºC for 4 h.

Coating CNTs on substrate surface

For synthesis of CNTs, it was used from a fixed bed flowed reactor [44]. The reactor which was composed of a ceramic boat containing 0.1 g of $BaCe_{0.2}Fe_{11.8}O_{19}$ powder as substrate (catalyst) was placed in a horizontal quartz tube with an external diameter of 50 mm, an internal diameter of 46 mm and a length of about 880 mm. After purging with argon for 30 min, the methane stream was opened for 60 min with a rate of 150 mL/min. The decomposition of methane on the surface of substrate was carried out at nearly 1000 °C. As a result, the growth of carbon nanotubes on $BaCe_{0.2}Fe_{11.8}O_{19}$ particles occurs. After this step, the methane stream was stopped and argon stream was opened until the temperature reached to room temperature. Finally, the prepared nanocomposite was collected for further analysis. The entire scheme of the coating CNTs on substrate surface based on CVD procedure was shown in Scheme 1.

Preparation of sample for microwave absorption characteristics

For microwave analysis, the specimens were prepared by mixing carbon nanocomposite with paraffin wax at a ratio of 40 % (w/w). The homogeneous mixtures were prepared and were pressed into rectangular cubic shaped molds with length 22.86 mm, width 10.16 mm, and 2-3 mm thicknesses. An Agilent 8510C network analyzer was employed to measure the complex permittivity, complex permeability, and reflection loss (*RL*) in the frequency range of 8.0–12.0 GHz.

RESULTS AND DISCUSSION

Characterization of nanocomposite

The typical XRD patterns of prepared samples were shown in Fig. 1. The XRD pattern of pure $BaFe_{12}O_{19}$ shows a crystalline phase (Fig. 1a). The positions and relative intensities of all peaks were typically indexed as M-type hexaferrite. The peaks match well with the (110), (107), (114), (203), (205), (206), (217), (2011), and (220) planes of the standard XRD data for the structure of hexaferrite [Joint Committee on Powder Diffraction Standards (JCPDS card no. 043-0002]. Fig. 1b show XRD pattern of Ce-substituted barium ferrite. In comparison with Fig. 1a, a miniority second phase of cerium oxide (CeO_2) was appeared, but doping by Ce does not change the crystalline structure of $BaFe_{12}O_{19}$ and show that Ce was substituted into the crystal lattice of barium ferrite. In this pattern, the peaks at 2θ of 28.7^0, 47.0^0, and 62.6^0 are corresponding to CeO_2. The secondary phase may be responsible for the microwave properties of this sample. Also in Fig. 1c, the diffraction pattern exhibits characteristic peaks of CNTs and $BaCe_{0.2}Fe_{11.8}O_{19}$. The XRD pattern of nanocomposite reflects a peak at 2θ of 26.4^0, which is the typical Bragg peak of CNTs and can be indexed to the (002) reflection of CNTs [45]. The presence of carbon nanotube and bariumferrite peaks reflects that the $BaCe_{0.2}Fe_{11.8}O_{19}$/CNTs nanocomposite was well formed.

Fig. 2a indicates the SEM image of $BaCe_{0.2}Fe_{11.8}O_{19}$/CNTs nanocomposite. It can be observed that CNTs were dispersed on the surface of Ce-substituted barium ferrite. Also, the mapping image in Fig. 2b shows that CNTs were deposited on the surfaces of the $BaCe_{0.2}Fe_{11.8}O_{19}$.

Electromagnetic parameters analysis

The magnetism of the particles

The magnetic properties of prepared samples were measured at room temperature with a VSM in an applied field from -10 kOe to +10 kOe. Fig. 3 shows hysteresis curves of Ce-substituted barium ferrite (a), and $BaCe_{0.2}Fe_{11.8}O_{19}$/CNTs nanocomposite (b). It is also

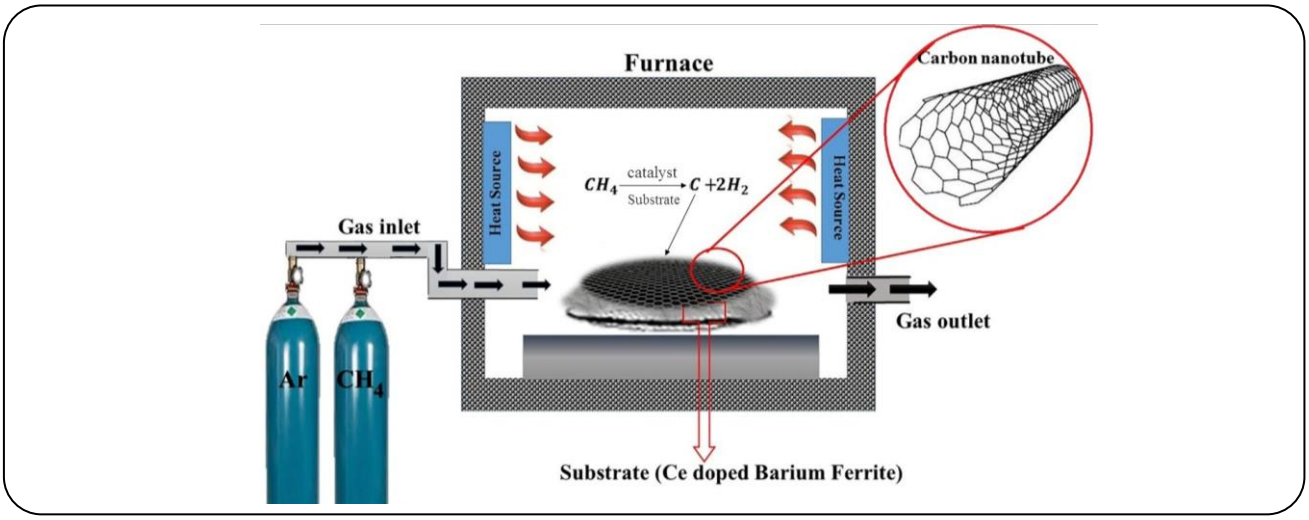

Scheme 1: Schematic illustration of the synthesis of carbon nanotubes on cerium-substituted barium ferrite substrate by chemical vapor deposition technique.

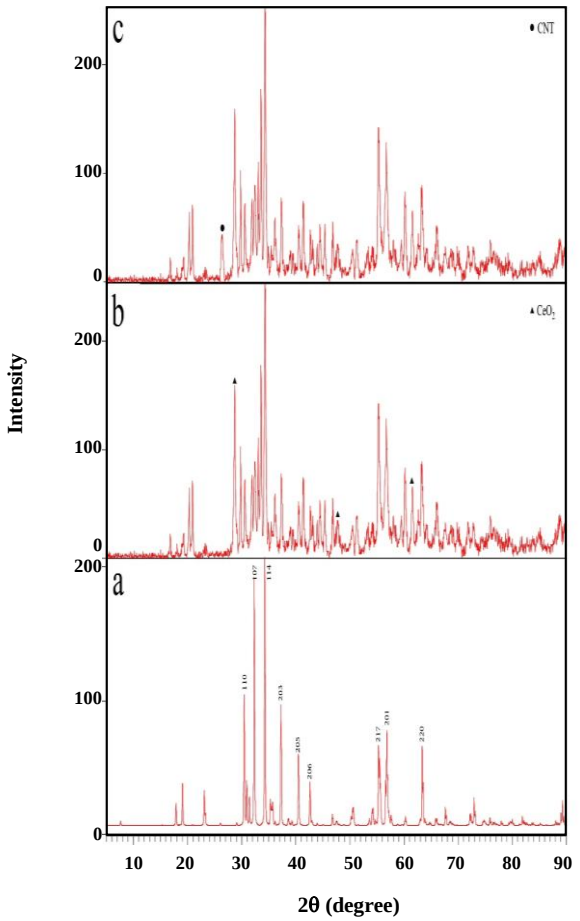

Fig. 1: The XRD patterns of the as-prepared a) $BaFe_{12}O_{19}$, b) $BaCe_{0.2}Fe_{11.8}O_{19}$ and c) $BaCe_{0.2}Fe_{11.8}O_{19}$/CNTs nanocomposite.

clearly seen that the value of saturation magnetization (*Ms*) decreases from 98.56 $emug^{-1}$ for Ce-substituted barium ferrite to 82.59 $emug^{-1}$ for nanocomposite. This could be attributed to the extistence of CNTs in nanocomposite. The saturation magnetization of carbon nanotubes in an applied field of 5 kOev is about 0.03 emu/g and consequently the magnetic properties are very weak and CNTs have diamagnetic properties [46].

Permittivity (ε) and permeability (μ) analysis

Complex permittivity and permeability (including real and imaginary parts) of a material have vital role in determining its electromagnetic wave absorption. Fig. 4 represents the real (ε') and imaginary (ε'') parts of the complex permittivity ($\varepsilon = \varepsilon' - j\varepsilon''$) and the real ($\mu'$) and imaginary ($\mu''$) parts of the complex permeability ($\mu = \mu' - j\mu''$) for $BaCe_{0.2}Fe_{11.8}O_{19}$. The ε' shows the stored energy via polarization mechanisms and ε'' represents the loss of energy via relaxation mechanisms. The μ' represents stored magnetic energy via the alignment of magnetic dipoles along the direction of the magnetic field and μ'' is the magnetic loss term, which is mainly due to ferromagnetic resonance. It can be observed in Fig 4a that the ε' increased from 1.0 to 2.5 by increasing frequency, whereas, the ε'' values approximately showed a broad peak in the range of 8–12 GHz, and had a peak value of 1.73 at 12.0 GHz. Also, it can be observed in Fig. 4b that the imaginary part of permeability (μ'') increases by increasing frequency and presents a peak with a value of

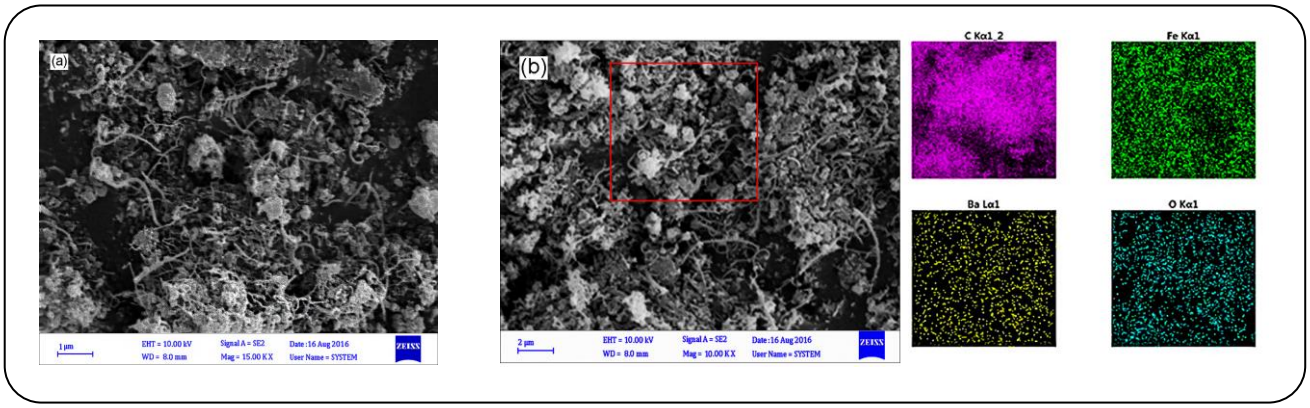

Figure 2: a) SEM image of $BaCe_{0.2}Fe_{11.8}O_{19}$/CNTs nanocomposite and b) EDX-elemental mapping images

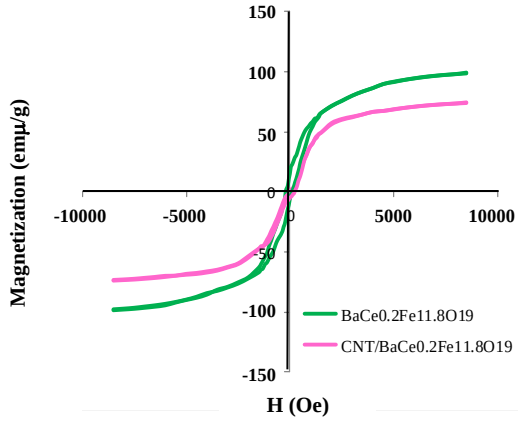

Fig. 3: The hysteresis loops of the $BaCe_{0.2}Fe_{11.8}O_{19}$/CNTs nanocomposite.

0.969 at 9.9 GHz, and then decreases, while the real part of complex permeability (μ') has an obviously decreasing trend in the range from 8.0-12.0 GHz. Because the ionic radius of Ce^{3+} is greater than that of Fe^{3+}, the substitution of Ce^{3+} ion for Fe^{3+} ion induces lattice defects, which result in increasing magnetic and dielectric loss.

As seen from the Fig. 5, significant increases have been occurred in both real and imaginary parts of permittivity, when CNTs deposited on surface $BaCe_{0.2}Fe_{11.8}O_{19}$. In $BaCe_{0.2}Fe_{11.8}O_{19}$/CNTs nanocomposite interfacial polarization of space charges at interface produces a nanoscale capacitor leading to an enhancement in the real part of permittivity (ε'). Also, for nanocomposite, the value of ε'' was higher than that of $BaCe_{0.2}Fe_{11.8}O_{19}$. In $BaCe_{0.2}Fe_{11.8}O_{19}$ /CNTs nanocomposite, ε'' is higher due to the presence of highly dielectric CNTs, and shows a great change from 0.82 at 8.2 GHz to 2.16 at 12.0 GHz. In fact, the relaxation mechanisms which are responsible for dielectric loss will be suppressed by increasing the frequency and therefore the loss term of permittivity decreases.

It can be seen that there exist frequency ranges in which the permittivity shows resonant characteristics with high loss. These ranges can be found around 10.9 and 12 GHz for ε'' which are related to two local minimums at these frequencies in ε'' curve. Also, in Fig. 5 are shown parts of the complex permeability (μ). The absolute values of μ' and μ'' for $BaCe_{0.2}Fe_{11.8}O_{19}$ /CNTs nanocomposite were higher than that of $BaCe_{0.2}Fe_{11.8}O_{19}$, which could be interpreted via protection of magnetic properties of $BaCe_{0.2}Fe_{11.8}O_{19}$ by the CNTs in the frequency range of experiment.

Microwave absorbing properties (Reflection loss calculation)

The microwave absorption ability of the samples was evaluated by measuring their reflection loss. All samples were poured into a standard X band wave guide. The electromagnetic fields were generated and recorded using two-port vector network analyzer. The Reflection Loss (RL) of the normal incident EM wave at the absorber surface can be defined as the ratio of the reflected power to the incident power by testing the absorbers backed by a perfect electronic conductor. Moreover, according to the transmission line theory [47], for a single-layer absorbing material, the *RL* of the normal incident EM wave at the absorber surface is given as follow [48]:

$$Z_{in} = \sqrt{\frac{\mu_r}{\varepsilon_r}} \tanh\left(\frac{j2\pi fd}{c}\sqrt{\mu_r \varepsilon_r}\right) \quad (1)$$

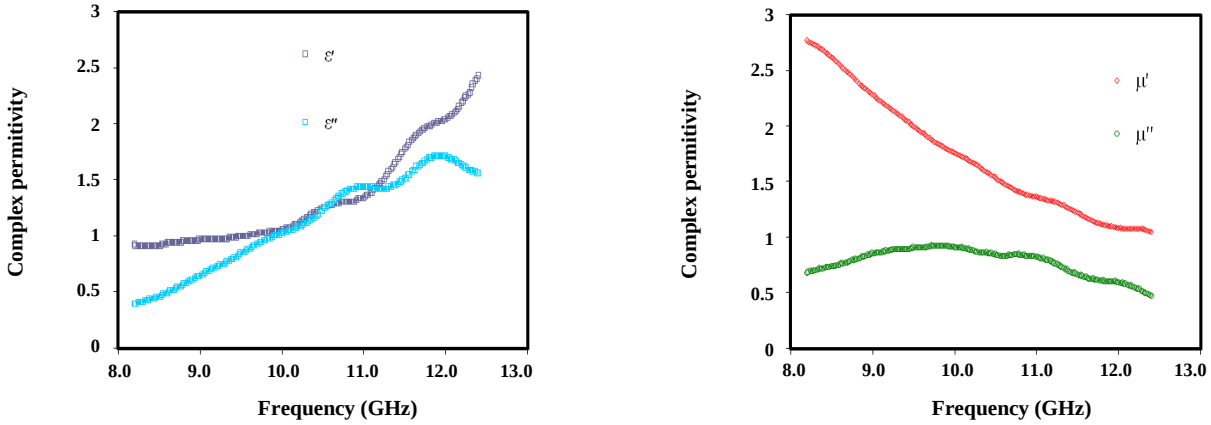

Fig. 4: a) Frequency dependence of complex permittiity, and b) Frequency dependence of complex permeability for $BaCe_{0.2}Fe_{11.8}O_{19}$..

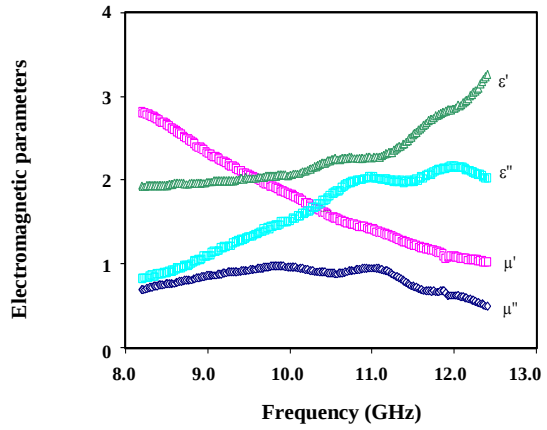

Fig. 5: Frequency dependence of electromagnetic parameters for $BaCe_{0.2}Fe_{11.8}O_{19}$/CNTs nanocomposite.

$$RL = 20\log\left|\frac{Z_{in} - Z_o}{Z_{in} + Z_o}\right| \quad (2)$$

Where Z_{in} is the input impedance of the absorber, Z_0 is the impedance of free space, ε_r and μ_r are respectively the relative complex permeability and permittivity, f is the frequency of microwaves, d is the thickness of the absorber, and c is the velocity of light in free space. The thickness of the sample is one of major factors affecting both the intensity of the *RL* peak and the value of the frequency at the *RL* minimum.

The reflection loss for both $BaCe_{0.2}Fe_{11.8}O_{19}$ and $BaCe_{0.2}Fe_{11.8}O_{19}$/CNTs nanocomposite in different layer thicknesses was calculated using Eqs.1 and 2 and shown in Fig. 6. For $BaCe_{0.2}Fe_{11.8}O_{19}$, the bandwidth with RL more than -10 dB reached more than 1GHz at a matching thickness of 4 mm. It can be seen that a maximum reflection loss value of -37.80 dB was observed at 10.6 GHz with a matching thickness of 4 mm. These results suggested that the doped-ferrite has an attractive potential microwave application. Compared with pure M-type barium ferrite, usually with a high natural ferrite ferromagnetic resonance frequency, the microwave absorbing property of the doped one is improved in the frequency band of 8–12 GHz [49].

As shown in Fig. 6, the effect of CNTs on the electromagnetic wave absorption properties is clearly seen from the figure. As seen from Fig. 6, the RL for $BaCe_{0.2}Fe_{11.8}O_{19}$/CNTs nanocomposite increases towards lower frequencies with increasing the absorber thickness. The maximum RL of about -49.61 dB is obtained for 2.5 mm thickness. There are two distinct absorption peaks in each thickness which indicates both dielectric and magnetic loss mechanisms in nanocomposite the bandwidth is defined as the frequency width for which the reflection loss is more than -20 dB. Such wide absorption widths and high absorption loss peaks indicate the potential for use in microwave applications. The maximum reflection loss of this band is -49.61 dB at the matching frequency of 9.0 GHz with a matching thickness of 2.5 mm. It is deduced from these graphs that with increasing carbon nanotube content in the nanocomposite, the bandwidth as well as the reflection loss values increase. The real and imaginary parts of the permittivity are enhanced on incorporation of CNTs [50]. It is well indicated from the graphs that with an increase in carbon nanotube content in nanocomposite, the bandwidth and reflection loss values were enhanced. The maximum of reflection loss is increased from -36.28 dB

Table 1: Comparison of electromagnetic parameters of the proposed method with some of the methods reported in literature.

Sample	Matching thickness (mm)	Matching frequency (GHz)	Optimal RL (dB)	Bandwidth (GHz) (RL<-10dB)	Bandwidth (GHz) (RL<-20dB)	Reference
Ce-doped barium hexaferrite	10	10.3	-16.43	1.0	-	[25]
$BaCe_{0.05}Fe_{11.95}O_{19}$	5.0	11.3	-31.52	2.9	1.0	[26]
Fe3O4/CNTs	-	10.6	-27	1.2	0.4	[30]
Barium ferrite/CNTs	3.0	10.5	-30.79	4.0	1.0	[32]
Strontium ferrite/CNTs	1.5	9.7	-29	3.0	1.0	[33]
$BaCe_{0.2}Fe_{11.8}O_{19}$/CNTs nanocomposite	2.5	9.0	-49.61	4.2	2.1	This work

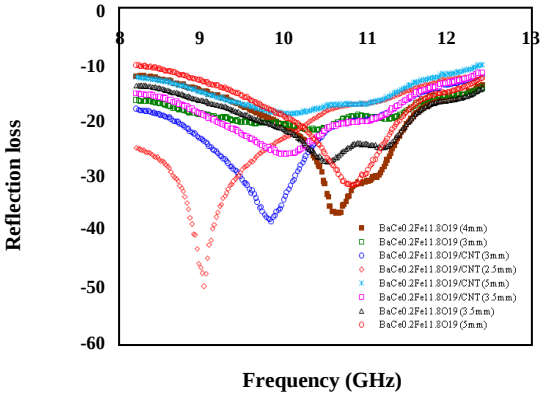

Fig. 6: Frequency dependence of electromagnetic parameters for $BaCe_{0.2}Fe_{11.8}O_{19}$/CNTs nanocomposite.

for $BaCe_{0.2}Fe_{11.8}O_{19}$ to -49.61 dB for nanocomposite coated with CNTs. Thus, the microwave absorption is improved for the $BaCe_{0.2}Fe_{11.8}O_{19}$/CNTs nanocomposite, because of the better match between the dielectric and magnetic losses caused by the presence of CNTs in nanocomposite.

CONCLUSIONS

In this work, a new approach was used for preparation of $BaCe_{0.2}Fe_{11.8}O_{19}$/CNTs nanocomposite by CVD method. The VSM results indicated that this nanocomposite has magnetic properties. The maximum reflection loss for nanocomposite was -49.61 dB at the matching frequency of 9.0 GHz for 2.5 mm thickness. Also the bandwidth in 90% power absorption and 99% power absorption can be obtained 4.2 GHz and 2.1 GHz, respectively. Also, the bandwidth and reflection loss values were enhanced with appropriate thickness. The electromagnetic parameters of $BaCe_{0.2}Fe_{11.8}O_{19}$/CNTs nanocomposite were better or comparable to some of the reported works. A comparison of the results is given in Table 1. As reported in Table 1, electromagnetic parameters at a same thickness improved due to presence of CNTs. Therefore, proposed method suggests that $BaCe_{0.2}Fe_{11.8}O_{19}$/CNTs nanocomposite can be used as a good radar absorption material in microwave region.

Received : Jun. 9, 2018 ; Accepted : Oct. 22, 2018

REFERENCES

[1] Huo J., Wang L, Yu H., Polymeric Nanocomposites for Electromagnetic Wave Absorption, *J. Mater. Sci.*, **44**: 3917-3927 (2009).

[2] Xu Y., Yan Z. Zhang D., Microwave Absorbing Property of a Hybrid Absorbent with Carbonyl Irons Coating on the Graphite, *Appl. Surf. Sci.*, **356:** 1032–1038 (2015).

[3] Wu H., Qu S., Lin K., Qing Y., Wang L., Fan Y., Fu Q., Zhang F., Enhanced Low-Frequency Microwave Absorbing Property of SCFs@ TiO_2 Composite, *Powder Technol.*, **333**: 153-159 (2018).

[4] Wu H., Wu G., Wang L., Peculiar Porous α-Fe_2O_3, γ-Fe_2O_3 and Fe_3O_4 Nanospheres: Facile Synthesis and Electromagnetic Properties, *Powder Technol.*, **269**: 443–451 (2015).

[5] Qing Y., Zhou W., Luo F., Zhu D., Microwave Absorbing and Mechanical Properties of Carbonyl Iron/Epoxy-Silicone Coating, *J. Magn. Magn. Mater.*, **321**: 25-28 (2009).

[6] Wu G., Cheng Y., Ren Y., Wang Y., Wang Zh., Wu H., Synthesis and Characterization of γ-Fe_2O_3@C Nanorod-Carbon Sphere Composite and Its Application as Microwave Absorbing Material, *J. Alloy Compd.*, **652**: 346-350 (2015).

[7] Wu H., Wu G., Ren Y., Yang L., Wang L., Li X., Co^{2+}/Co^{3+} Ratio Dependence of Electromagnetic Wave Absorption in Hierarchical $NiCo_2O_4$-$CoNiO_2$ Hybrids, *J. Mater. Chem. C*, **3**: 7677–7690 (2015).

[8] Liu J.W., Che R.C., Chen H.J., Zhang F., Xia F., Wu Q.S., Wang M., Microwave Absorption Enhancement of Multifunctional Composite Microspheres with Spinel Fe_3O_4 Cores and Anatase TiO_2 Shells, *Small*, **8**: 1214–1221 (2012).

[9] Zhou M., Zhang X., Wei J.M., Zhao S.L., Wang L., Feng B.X., Morphology-Controlled Synthesis and Novel Microwave Absorption Properties of Hollow Urchin Like a-MnO_2 Nanostructures, *J. Phys. Chem. C*, **115**: 1398–140 (2011).

[10] Zhang T., Huang D., Yang Y., Kang F., Gu J., Fe_3O_4/Carbon Composite Nanofiber Absorber with Enhanced Microwave Absorption Performance, *Mater. Sci. Eng. B*, **178**: 1–9 (2013).

[11] Ren Y.L., Zhu C.L., Qi L.H., Gao H., Chen Y.J., Growth of G-Fe_2O_3 Nanosheet Arrays on Graphene for Electromagnetic Absorption Applications, *RSC Adv.*, **4**: 21510-21516 (2014).

[12] Zhou H., Wang J., Zhuanga J., Liu Q., A Covalent Route for Efficient Surface Modification of Ordered Mesoporous Carbon as High Performance Microwave Absorbers, *Nanoscale*, **5**: 12502-12511 (2013).

[13] Zhang P., Han X., Kang L., Qiang R., Liu W., Du Y., Synthesis and Characterization of Polyaniline Nanoparticles with Enhanced Microwave Absorption, *RSC Adv.*, **3:** 12694-12701 (2013).

[14] Adohi B.J.P., Mdarhri A., Prunier C., Haidar B., Brosseau C., A Comparison Between Physical Properties of Carbon Black-Polymer and Carbon Nanotubes polymer Composites, *J. Appl. Phys.*, **108:** 074108 (2010).

[15] Wu H., Wu G., Wu Q., Wang L., Facile Synthesis and Microwave Absorbability of C@ Ni–NiO Core–Shell Hybrid Solid Sphere and Multi-Shelled NiO Hollow Sphere, *Mater. Charact.*, **97:** 18-26 (2014).

[16] Alaei M., Simple Method for the Preparation of Fe_3O_4/MWCNT Nanohybrid as Radar Absorbing material (RAM), *Iran. J. Chem. Chem. Eng. (IJCCE)*, **37**(6): 9-14 (2018).

[17] Sugimoto S., Kondo S., Okayama K., Book D., Kagotani, T., Homma, M., M-Type Ferrite Composite as a Microwave Absorber with Wide Bandwidth in the GHz Range, *IEEE Trans. Magn.*, **35:** 3154–3156 (1999).

[18] Cho H.S., Kim S.S., M-hexaferrites with Planar Magnetic Anisotropy and Their Application to High-Frequency Microwave Absorbers, *IEEE Trans. Magn.*, **35:** 3151-3153 (1999).

[19] Lisjak D., Bobzin K. Richardt K., Begard M., Bolelli G., Lusvarghi L., Hujanen A., Lintunen P., Pasquale M., Olivetti E., Drofenik M. Schlafer T., Preparation of Barium Hexaferrite Coatings Using at Mospheric Plasma Spraying, *J. Eur. Ceram. Soc.*, **29:** 2333–2341 (2009).

[20] Pardavi-Horvath M., Microwave Applications of Soft Ferrites, *J. Magn. Magn. Mater.*, **215–216:** 171–183 (2000).

[21] Gairola S.P., Verma V., Singh A., Purohit L.P., Kotnala R.K., Modified Composition of Barium Ferrite to Act as a Microwave Absorber in X-Band Frequencies, *Solid State Commun.*, **150:** 147–151 (2010).

[22] Liu Y., Drew M.G.B., Wang,J., Zhang M. Liu Y., Efficiency and Purity Control in the Preparation of Pure and/or Aluminum-Doped Barium Ferrites by Hydro-Thermal Methods Using Ferrous Ions as Reactants, *J. Magn. Magn. Mater.*, **322:** 366-374 (2010).

[23] Ahmed M.A., Okasha N. Kershi R.M., Influence of Rare-Earth Ions on the Structure and Magnetic Properties of Barium W-Type Hexaferrite, *J. Magn. Magn. Mater.*, **320**: 1146–1150 (2008).

[24] Gu Y.Y., Tan X.P., Liang S.Q., Sang S.B., Effects of La^{3+} Doping on MnZn Ferrite Nanoscale Particles Synthesized by Hydrothermal Method, *J. Cent. South. Univ. Technol.*, **11**: 166-168 (2004).

[25] Mosleh Z., Kameli P., Poorbaferani A., Ranjbar M., Salamati H., Structural, Magnetic and Microwave Absorption Properties of Ce-doped Barium Hexaferrite, *J. Magn. Magn. Mater.*, **397**: 101-107 (2016).

[26] Chang S., Kangning S. Pengfei, C., Microwave Absorption Properties of Ce-Substituted M-Type Barium Ferrite, *J. Magn. Magn. Mater.*, **324:** 802–805 (2012).

[27] Che R.C., Peng L.M., Duan X.F., Chen Q., Liang X.L., Microwave Absorption Enhancement and Complex Permittivity and Permeability of Fe Encapsulated Within Carbon Nanotubes, *Adv. Mater.*, **16**: 401-405 (2004).

[28] Lin H., Zhu H., Guo H., Yu L., Investigation of the Microwave-Absorbing Properties of Fe-Filled Carbon Nanotubes, *Mater. Lett.*, **61**: 3547–3550 (2007).

[29] Roberts J.A., Imholt T., Ye Z., Electromagnetic Wave Properties of Polymer Blends of Single Wall Carbon Nanotubes Using a Resonant Microwave Cavity as a Probe, *J. Appl. Phys.*, **95**: 4352–4356 (2004).

[30] Hekmatara H., Seifi M., Forooraghi K., Microwave Absorption Property of Aligned MWCNT/Fe_3O_4, *J. Magn. Magn. Mater.*, **346**: 186-191 (2013).

[31] Shakirzianov F.N., Han B., Kiaisec A.A., Cheparin V.P., "The Effect of Nanotubes on Electromagnetic Waves Absorption in Composite Radio Absorbing Materials on the Basis of Hexagonal Ferrites", *Proc. 9th Int. Conf. Prop. Appl. Dielectric Mater.*,1211–1214 (2009).

[32] He K., Yu L., Sheng L., An K., Ando Y., Zhao X., Doping Effect of Single-Wall Carbon Nanotubes on The Microwave Absorption Properties of Nanocrystalline Barium Ferrite, *J. J. Appl. Phys.*, **49:** 125101-125105 (2010).

[33] Zhao D.X., Li Q.L., Ye Y., Zhang C.R., Synthesis and Characterization of Carbon Nanotubes Decorated with Strontium Ferrite Nanoparticles, *Synth. Met.*, **160**: 866-870 (2010).

[34] Ghasemi A., Shirsath S.E., Liu X., Morisako A., Enhanced Reflection Loss Characteristics of Substituted Barium Ferrite/Functionalized Multi-Walled Carbon Nanotube Nanocomposites, *J. Appl. Phys.*, **109**: 07A507 (2011).

[35] Ghasemi A., Javadpour S., Liu X., Morisako A., Magnetic and Reflection Loss Characteristics of Substituted Barium Ferrite/Functionalized Multiwalled Carbon Nanotube, *IEEE Trans. Magn.*, **47**: 4310-4313 (2011).

[36] Yu Y., Qu S., Zang D., Wang L., Wu H., Fast Synthesis of Pt Nanocrystals and Pt/Microporous La_2O_3 Materials Using Acoustic Levitation, *Nanoscale Res. Lett.*, **13:** 50 (2018).

[37] Qu S., Yu Y., Lin K., Liu P., Zheng C., Wang L., Xu T., Wang Zh., Wu H., Easy Hydrothermal Synthesis of Multi-Shelled La_2O_3 Hollow Spheres for Lithium-Ion, *J Mater Sci: Mater Electron.*, **29**: 1232-1237 (2018).

[38] Koziol K., Boskovic B.O., Yahya N., Synthesis of Carbon Nanostructures by CVD, Carbon and Oxide Nanostructures, *Adv. Struct. Mater.*, **5**: 23–49 (2010).

[39] Bahrami B., Khodadadi A., Mortazavi Y. Esmaieli M., Short Time Synthesis of High Quality Carbon Nanotubes with High Rates by CVD of Methane on Continuously Emerged Iron Nanoparticles, *Appl. Surf. Sci.*, **257**: 9710–9716 (2011).

[40] Oliveira H.A., Franceschini D.F., Passos F.B., Support Effect on Carbon Nanotube Growth by Methane Chemical Vapor Deposition on Cobalt Catalysts, *J. Braz. Chem. Soc.*, **23:** 868-879 (2012).

[41] Rashidi A., Mortazavi Y., Khodadadi A., The Preparation of Bamboo-Structured Carbon Nanotubes with the Controlled Porosity by CVD of Acetylene on Co-Mo/MCM-41, *Iran. J. Chem. Chem. Eng. (IJCCE)*, **25**(3): 9-13 (2006).

[42] Zhou W., Han Z., Wang J., Zhang Y., Jin Z., Sun Z., Zhang Y., Yan C., Li Y., Copper Catalyzing Growth of Single-Walled Carbon Nanotubes on Substrates, *Nano Lett.*, **6**: 2987-2990 (2006).

[43] Uchino T., Bourdakos K.N., Ashburn C.H.deGroot P., Kiziroglou M.E., Dilliway G., Smith D.C., Metal Catalyst-Free Low-Temperature Carbon Nanotube Growth on SiGe Islands, *Appl. Phys. Lett.*, **86:** 233110 (2005).

[44] Alijani H., Beyki M.H., Shariatinia Z., Bayat M., Shemirani F., A New Approach for One Step Synthesis of Magnetic Carbon Nanotubes/Diatomite Earth Composite by Chemical Vapor Deposition Method: Application for Removal of Lead Ions, *Chem. Eng. J.*, **253**: 456-463(2014).

[45] Ghasemi A., Remarkable Influence of Carbon Nanotubes on Microwave Absorption Characteristics of Strontium Ferrite/CNT Nanocomposites, *J. Magn. Magn. Mater.*, **323**: 3133-3137 (2011).

[46] Li Y., Huang Y., Qi S., Niu L., Zhang Y. Wu Y., Preparation, Magnetic and Electromagnetic Properties of Polyaniline/Strontium Ferrite/Multiwalled Carbon Nanotubes Composite, *Appl. Surf. Sci.*, **258**: 3659-3666 (2012).

[47] Ramo S., Whinnery J.R., Van Duzer T., "Fields and Waves in Communication Electronics", 3rd ed., John Wiley & Sons, Inc., New Jersey, USA (1994).

[48] Naito Y., Suetake K., Application of Ferrite to Electromagnetic Wave Absorber and Its Characteristics, *IEEE Trans. Microw. Theory. Tech.*, **19:** 65–72 (1971).

[49] Liu K.H., Li D.R., Liu T.C., Zhang L., Lu Z.C., Zhou, S.X., Effect of Fe-Based Amorphous Flakes Distribution on Electromagnetic Properties of Microwave Absorbers, *Metallic Funct. Mater.*, **17**: 1–4 (2010).

[50] Ghasemi A., Hossienpour A., Morisako A., Saatchi A., Salehi M., Electromagnetic Properties and Microwave Absorbing Characteristics of Doped Barium Hexaferrite, *J. Magn. Magn. Mater.*, **302**: 429–435 (2006).